Notch signaling molecule is involved in the invasion of MiaPaCa2 cells induced by $CoCl_2$ via regulating epithelial-mesenchymal transition

DING-WEI CHEN[1], HONG WANG[2], YA-FANG BAO[3] and KUN XIE[1]

[1]Department of General Surgery, Sir Run Run Shaw Hospital, Zhejiang University School of Medicine, Hangzhou, Zhejiang 310016; [2]Zhejiang Medical College, Hangzhou, Zhejiang 310053; [3]Caihe Street Community Health Service Center, Hangzhou, Zhejiang 310016, P.R. China

Received November 23, 2016; Accepted December 5, 2017

DOI: 10.3892/mmr.2018.8502

Abstract. Pancreatic cancer exhibits a high mortality rate resulting from metastasis and there is currently no effective treatment strategy. Hypoxia serves an important role in cancer cells, where cellular metabolic rate is high. The underlying mechanisms that trigger hypoxia and the invasion of pancreatic cancer cells remain unknown. Investigation of the importance of hypoxia in the invasion of pancreatic cancer cells for potential, novel treatment strategies is of primary concern. Cell Counting Kit-8 assay, invasion assay, western blotting and reverse transcription-quantitative polymerase chain reaction were used to investigate invasion and epithelial mesenchymal transition (EMT) and the expression of Notch1 in MiaPaCa2 cells treated with cobalt II chloride ($CoCl_2$). Hypoxia-inducible factor 1α (HIF-1α) small interfering (si)RNA and Notch1 inhibitor N-[N-(3,5-Difluorophenacetyl)-L-alanyl]-S-phenylglycine t-butyl ester (DAPT) were also selected to investigate these mechanisms. Data indicated that $CoCl_2$ increased the invasion ability and altered EMT in MiaPaCa2 cells. $CoCl_2$ regulated the expression of HIF-1α and Notch1 in MiaPaCa2 cells. In addition, HIF-1α siRNA inhibited the effects of $CoCl_2$ on the expression of Notch1 and decreased Snail, EMT and invasion in MiaPaCa2 cells. DAPT increased the expression of epithelial-cadherin and decreased the content of neural-cadherin, Snail and invasion in MiaPaCa2 cells in the presence or absence of $CoCl_2$. $CoCl_2$ promoted invasion by stimulating the expression of HIF-1α and regulating the expression of Notch1 and EMT in MiaPaCa2 cells. Targeting the Notch1 signaling molecule may be a novel treatment strategy for the prevention and treatment of pancreatic cancer.

Correspondence to: Dr Ding-Wei Chen, Department of General Surgery, Sir Run Run Shaw Hospital, Zhejiang University School of Medicine, 3 East Qingchun Road, Hangzhou, Zhejiang 310016, P.R. China
E-mail: 11118152@zju.edu.cn

Key words: pancreatic cancer, cobalt II chloride, epithelial-mesenchymal transition, hypoxia-inducible factor 1α, Notch1

Introduction

Pancreatic cancer, one of the most frequently occurring cancers in the world, is a devastating malignant disease with a median survival of 3-6 months and a 5-year survival rate of less than 5% (1-4). Despite improvements in surgical techniques and adjuvant medical therapy, pancreatic cancer remains a threat to human health. Previous data demonstrated that 48,960 people were estimated to be diagnosed with pancreatic cancer in 2015, and 40,560 people would succumb to pancreatic cancer in the United States (5). It is therefore urgent to discover the mechanism of progression of pancreatic cancer, and thereby contribute to investigating novel therapeutic strategies for preventing and treating pancreatic cancer.

A significant feature of cancer is a high rate of cellular metabolism, which results in a lack of oxygen and creates a hypoxic environment for cancer cells (6). Hypoxia serves an important role in the development of cancer and is a common condition in the microenvironment of solid tumors. Hypoxia promotes Rab5 activation and regulates cell migration and invasion in lung carcinoma, breast cancer and melanoma (6). A decline in oxygen may additionally result in cancer cells resistant to radiotherapy and anti-cancer drugs, by inducing the expression of various anti-apoptotic genes (7-10). Hypoxia affects the maintenance of the characteristic belonging to cancer stem cells, resulting in cancer recurrence and progression (11). It has been reported that pancreatic cancer is also associated with hypoxia, which promotes cancer progression (12), however the mechanism by which hypoxia affects the development in pancreatic cancer remains unclear.

The high metastatic rate is the reason that pancreatic cancer possesses a poor prognosis. In the present study, the role of hypoxia in the invasion of pancreatic cancer stem cells *in vitro* and its mechanism was investigated, which contributed to research for a novel potential treatment strategy for pancreatic cancer.

Cobalt II chloride ($CoCl_2$), an inorganic compound, may be used to provide a hypoxic environment (13), which is similar

to the normal environment of cancer cells and has been used to investigate the role of hypoxia in the progression of cancer development (14).

Epithelial-mesenchymal transition (EMT) is associated with metastasis, which alters the cytoskeleton and regulates migration and invasion of cancer cells (15,16). Hypoxia-inducible factor (HIF)-1α affects EMT resulting in an increase in migration and invasion from the primary tumor (17-19) and affects the Notch signaling pathway, which is very important in regulating cell behaviors, including proliferation, apoptosis, and migration and invasion (20-22). It has been reported that the Notch signaling pathway could regulate the content of epithelial (E)-cadherin (a marker of epithelial cells) and neural (N)-cadherin (a marker of mesenchymal cells) by altering the expression of Snail, leading to EMT (23,24). However, whether HIF-1α induced by $CoCl_2$ increases EMT to promote invasion via the Notch signaling pathway in pancreatic cancer stem cells is unclear.

Materials and methods

Reagents. Anti-E-cadherin antibody, anti-N-cadherin antibody, anti-Snail antibody, anti-HIF-1α antibody, anti-Notch1 antibody, anti-β-actin antibody and horseradish peroxidase-conjugated anti-rabbit antibody, and N-[N-(3,5-Difluorophenacetyl)-L-alanyl]-S-phenylglycine t-butyl ester (DAPT) were purchased from Santa Cruz Biotechnology, Inc., (Dallas, TX, USA). $CoCl_2$ was purchased from Sigma-Aldrich; Merck KGaA (Darmstadt, Germany).

Cell culture. MiaPaCa2 cells used in the present study were obtained from American Type Culture Collection (Manassas, VA, USA). The cell line was maintained in Dulbecco's modified Eagle's medium (DMEM; HyClone; GE Healthcare, Logan, UT, USA) supplemented with 10% (v/v) fetal bovine serum (FBS; Invitrogen; Thermo Fisher Scientific, Inc., Waltham, MA, USA) and 1% (v/v) penicillin/streptomycin (Invitrogen; Thermo Fisher Scientific, Inc.), incubated at 37˚C in a carbon dioxide incubator.

Cell viability assay. The effects of $CoCl_2$ on the growth of MiaPaCa2 cells were detected using a Cell Counting Kit (CCK)-8. A total of $1x10^4$ cells per well in 96-well plate were treated with or without $CoCl_2$ (0.08 or 0 mM, respectively) in the presence or absence of HIF-1α small interfering (si)RNA (5 or 0 μg, respectively) or DAPT (0.01 or 0 mM, respectively). In addition, the control cells were treated with an equal volume (100 μl) of DMEM. Cell viability was detected at 24 h following treatment with $CoCl_2$. A solution containing WST-8 (2-(2-methoxy-4-nitrophenyl)-3-(4-nitrophenyl)-5-(2,4-disulfophenyl)-2H-tetrazolium, monosodium salt) was added to cells according to the manufacturer's protocol and absorbance was detected at a wavelength of 450 nm. All experiments were performed in triplicate.

Invasion assay. Cell invasion was analyzed using the BD BioCoat™ Matrigel™ Invasion Chamber (BD Biosciences, Franklin Lakes, NJ, USA), according to the manufacturer's protocol. Individual cells were plated in the upper insert, at a density of $1.5x10^5$ cells/ml in a 24-well chamber, in serum-free DMEM containing 10% FBS as a chemoattractant was added to the wells. Then cells were treated with or without $CoCl_2$ (0.08 or 0 mM, respectively) for 24 h in the presence or absence of HIF-1α siRNA (5 or 0 μg, respectively) or DAPT (0.01 or 0 mM, respectively). Invaded cells were stained by 0.5% crystal violet (25˚C for 1 h; Beijing Solarbio Science & Technology Co., Ltd., Beijing, China) according to the manufacturer's protocol. Invaded cells were counted in three suitable areas by stereoscopic microscope (BH-2; Olympus Corporation, Tokyo, Japan) at x200 magnification.

Hematoxylin and eosin (H&E) staining. H&E staining using the kit (Beyotime Institute of Biotechnology, Jiangsu, China), according to the manufacturer's protocol. In brief, MiaPaCa2 cells ($1x10^5$ cells/ml) were treated with or without $CoCl_2$ for 24 h in the presence or absence of HIF-1α siRNA or DAPT, and then cells were stained with H&E (hematoxylin for 5 min at 25˚C, eosin for 2 min at 25˚C) and observed from five randomly selected microscopic visual fields (magnification, x200) by stereoscopic microscope (BH-2; Olympus Corporation).

RNA extraction and reverse transcription-quantitative polymerase chain reaction (RT-qPCR) assay. Total RNA was extracted from the cells with RNAiso plus reagent (Takara Biotechnology Co., Ltd., Dalian, China) following the manufacturer's protocol. The concentration of RNA was determined by a spectrophotometer. First-strand cDNA was synthesized using a Transcriptor First Strand cDNA Synthesis kit (Roche Diagnostics GmbH). The reaction was conducted using a 7500 Fast Real-time quantitative PCR System (Applied Biosystems; Thermo Fisher Scientific, Inc.). The SYBR® Fast qPCR Mix containing the fluorophore reagent, was obtained from Takara Biotechnology Co., Ltd. The qPCR amplification conditions were as follows: 50˚C for 2 min and 95˚C for 10 min, followed by 40 cycles of 95˚C for 10 sec, 58˚C for 10 sec, and 72˚C for 10 sec. The forward and reverse primer sequences qPCR for E-cadherin were: Forward, 5'-GAGAACGCATTGCCACATACAC-3' and reverse, 5'-AAGAGCACCTTCCATGACAGAC-3'; for N-cadherin were forward, 5'-CATCATCCTGCTTATCCTTG-3' and reverse, 5'-AAGTCATAGTCCTGGTCTTC-3'; for Snail were forward, 5'-TCGCTGCCAATGCTCATC-3' and reverse, 5'-CCTTTCCCACTGTCCTCATC-3'; for HIF-1α were forward, 5'-TCGGCGAAGTAAAGAATC-3' and reverse, 5'-TTCCTCACACGCAAATAG-3'; for Notch1 were forward, 5'-GACGCACAAGGTGTCTTC-3' and reverse, 5'-TTGCCCAGGTCATCTACG-3'; for GAPDH were forward, 5'-CACCCACTCCTCCACCTTTG-3' and reverse, 5'-CCACCACCCTGTTGCTGTAG-3'. The contents on RNA level were decided by $2^{-\Delta\Delta Cq}$ method (25).

Western blotting assay. Cells ($1x10^6$ cells/ml) were dissolved using the radioimmunoprecipitation assay lysis buffer (Beyotime Institute of Biotechnology) and the lysate was centrifuged at 10,000 x g at 4˚C for 30 min following incubation on ice for 50 min. Then, each sample containing 40 μg protein as subjected to 12% (w/v) SDS-PAGE and transferred to polyvinylidene fluoride transfer membranes (GE Healthcare, Chicago, IL, USA). Following blocking in 5% (w/v) skimmed milk (25˚C for 1 h), membranes were incubated (4˚C, overnight)

with anti-E-cadherin antibody (1:1,000; sc-7870; Santa Cruz Biotechnology), anti-N-cadherin antibody (1:1,000; sc-7939; Santa Cruz Biotechnology), anti-Snail antibody (1:1,000; sc-28199; Santa Cruz Biotechnology), anti-HIF-1α antibody (1:1,000; sc-10790; Santa Cruz Biotechnology), anti-Notch1 antibody (1:1,000; sc-9170; Santa Cruz Biotechnology) and anti-GAPDH antibody (1:1,000; sc-25778; Santa Cruz Biotechnology), and then incubated (25˚C for 1 h) with the horseradish peroxidase-conjugated anti-rabbit secondary antibody (1:5,000; sc-2004; Santa Cruz Biotechnology). Finally, proteins were detected by chemiluminescence (PerkinElmer, Inc., Waltham, MA, USA) and densitometric analysis used ImageJ software (1.8.0_112; National Institutes of Health, Bethesda, MD, USA).

siRNA. MiaPaCa2 cells were transfected with three different HIF-1α siRNA (siRNA1, siRNA2 and siRNA3) (sequences as 5'-GCCACATTCAGTATATATGA-3', 5'-GCCGCT CATTTATGAATA-3' and 5'-GGGCAATGAATGGAT GAAA-3' respectively), or negative control siRNA (5'-TTC TCCGAACGTGTCACGTTT-3',) using Lipofectamine® 2000 (Invitrogen; Thermo Fisher Scientific, Inc.). At subconfluent conditions, ~50% density, transfection reagents containing 12 pmol siRNA and 16 μl Lipofectamine® 2000 in a final volume of 1.6 ml with Opti-MEM I (Invitrogen; Thermo Fisher Scientific, Inc.) was added to each flask, and incubated for 48 h prior to culture with $CoCl_2$ (0.08 mM).

Statistical analysis. The statistical analysis was achieved by the SPSS 18.0 statistical software (SPSS, Inc., Chicago, IL, USA). All data were shown as the mean ± standard error (±S). The comparisons between two groups was conducted with the LSD method (least significant method) in the One-way analysis of variance method and $P<0.05$ was considered to indicate a statically significant difference.

Results

$CoCl_2$ increases the invasion of MiaPaCa2 cells. To investigate the effects of hypoxia on pancreatic cancer, MiaPaCa2 cells were cultured with $CoCl_2$, which creates a hypoxic-like-microenvironment, and their growth and invasion were measured by CCK-8 assay and invasion assay. Data indicated that $CoCl_2$ at different concentrations had various effects on the growth of MiaPaCa2 cells, a pancreatic cancer cell line (Fig. 1). When the concentration of $CoCl_2$ was 0.02 mM, it demonstrated little effect on the viability of MiaPaCa2 cells (Fig. 1C). When $CoCl_2$ reached 0.04 or 0.08 mM, it significantly increased cell viability in MiaPaCa2 cells ($P<0.01$; Fig. 1C). $CoCl_2$ (0.08 mM) increased the cell viability by 20%, compared with those cells not treated with $CoCl_2$ (Fig. 1C).

The effects of $CoCl_2$ at different concentrations on the invasion of MiaPaCa2 cells were analyzed using an invasion assay. Data demonstrated that $CoCl_2$ exhibited effects on the invasion of MiaPaCa2 cells (Fig. 1A and B). When $CoCl_2$ reached 0.08 mM the cell invasion rate significantly increased from 100-200%, two-fold, compared with 0 mM $CoCl_2$ ($P<0.001$; Fig. 1A and B). Once the concentration of $CoCl_2$ exceeded 0.08 mM, the increase in invasion reduced in a dose-dependent manner (Fig. 1A and B). According to the effects of $CoCl_2$ (0.08 mM) on cell viability and cell invasion, $CoCl_2$ increased the cell growth and the invasion of MiaPaCa2 cells.

$CoCl_2$ promotes EMT in MiaPaCa2 cells. Invasion ability is different between mesenchymal and epithelial cells resulting from a difference in the cytoskeleton, which allows cell types to be distinguished from one another. The marker of epithelial cells is E-cadherin, and N-cadherin marks mesenchymal cells, which means during EMT there is a decline in E-cadherin and an increase in N-cadherin.

To investigate whether $CoCl_2$ promoted invasion via regulating EMT, the morphology of MiaPaCa2 cells were detected by H&E staining following treatment with $CoCl_2$ (0.08 mM). The results of the present study demonstrated that $CoCl_2$ altered the morphology of MiaPaCa2 cells from epithelioid to spindle shaped, which is similar to the morphology of mesenchymal cells (Fig. 2A). Western blotting and RT-qPCR experiments demonstrated that $CoCl_2$ significantly decreased the expression of E-cadherin and significantly increased the content of N-cadherin on a transcriptional and translational level ($P<0.001$; Fig. 2B and C). Consequently, EMT induced by $CoCl_2$ may result in an increase in invasion of MiaPaCa2 cells.

To investigate the role of Snail in EMT and invasion induced by $CoCl_2$, the expression of Snail was detected by RT-qPCR and western blotting in MiaPaCa2 cells. It was observed that the mRNA and protein expression of Snail significantly increased in MiaPaCa2 cells treated with $CoCl_2$ (0.08 mM) compared with untreated cells ($P<0.001$; Fig. 2B and C). $CoCl_2$ may increase the expression of Snail, and then promote EMT, leading to an increase to invasion in MiaPaCa2 cells.

Knockdown of HIF-1α decreases the invasion of MiaPaCa2 cells induced by $CoCl_2$. $CoCl_2$ was used in the present study to imitate the hypoxia like microenvironment of cancer and HIF-1α expression was induced. To prove that $CoCl_2$ regulated EMT and invasion resulting from an increase in the expression of HIF-1α, the content of HIF-1α was measured in MiaPaCa2 cells by RT-qPCR and western blotting. Data indicated that $CoCl_2$ increased the expression of HIF-1α on a transcriptional and translational level (Fig. 2B and C). Then, HIF-1α siRNA was selected by RT-qPCR to identify the role of HIF-1α in MiaPaCa2 cells treated with $CoCl_2$. It was observed that HIF-1α siRNA decreased the expression of HIF-1α, particularly siRNA1, which significantly decreased the content of HIF-1α to 30% at 48 h and to 20% at 72 h ($P<0.001$; Fig. 3A). Data indicated that the knockdown of HIF-1α inhibited EMT and the invasion in MiaPaCa2 cells (Fig. 3B and C; Fig. 4). Additionally, HIF-1α siRNA inhibited the effects of $CoCl_2$ on the expression of Snail, EMT and invasion in MiaPaCa2 cells (Fig. 3B and C; Fig. 4). $CoCl_2$ imitated a hypoxic environment and increased the expression of Snail, and then induced EMT resulting in an increase in invasion by stimulating the expression of HIF-1α.

Notch1 inhibitor DAPT decreases the invasion of MiaPaCa2 cells induced by $CoCl_2$. Whether the Notch signaling pathway is involved in invasion mediated by HIF-1α in MiaPaCa2 cells

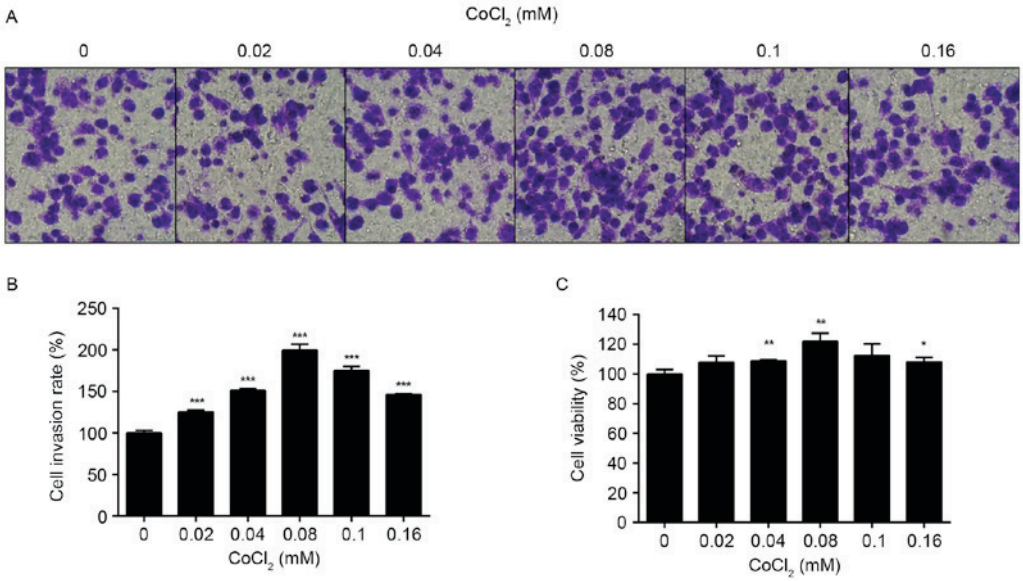

Figure 1. Effects of $CoCl_2$ on cell growth and invasion in MiaPaCa2 cells. (A) Cell invasion was detected in MiaPaCa2 cells following treatment with $CoCl_2$ at 0, 0.02, 0.04, 0.08, 0.10 and 0.16 mM for 24 h. Invaded cells were stained with crystal violet and observed from five randomly selected microscopic visual fields (magnification, x200). (B) Invaded cells were counted and expressed as cell invasion rate (%) compared with the untreated cells. (C) Cell viability was measured using Cell Counting Kit-8 assay and analyzed by the absorbance at a wavelength of 450 nm, following treatment with 0, 0.02, 0.04, 0.08, 0.10 and 0.16 mM $CoCl_2$ for 24 h. Data were representative of three independent experiments and expressed as the mean ± standard error of the mean. *P<0.05, **P<0.01, ***P<0.001 vs. control. $CoCl_2$, cobalt II chloride.

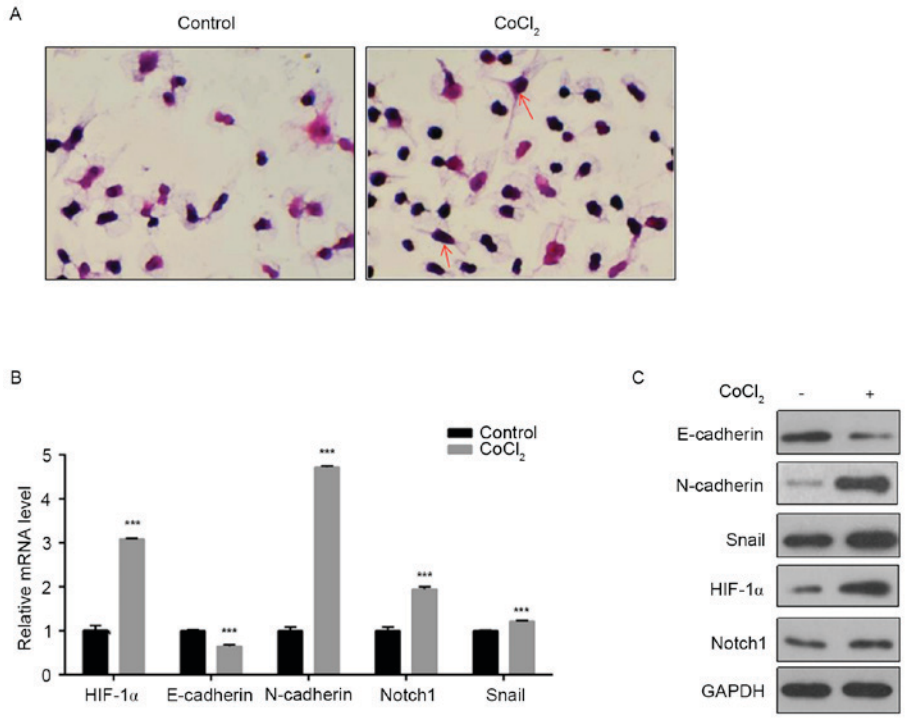

Figure 2. Effects of $CoCl_2$ on proteins involved in epithelial-mesenchymal transition in MiaPaCa2 cells. (A) The morphology of cells was detected by hematoxylin and eosin staining and observed from five randomly selected microscopic visual fields (magnification, x200) following treatment with or without $CoCl_2$ for 24 h. Red arrow represented cells with spindle shape. (B) The mRNA expression levels of E-cadherin, N-cadherin, Snail, HIF-1α, Notch1 in MiaPaCa2 cells treated with or without $CoCl_2$ for 24 h was detected using reverse transcription-quantitative polymerase chain reaction. (C) The protein content of E-cadherin, N-cadherin, Snail, HIF-1α, Notch1 in MiaPaCa2 cells treated with or without $CoCl_2$ for 24 h was detected by western blotting. GAPDH was included as mRNA-loading and protein-loading control. Data were representative of three independent experiments and expressed as the mean ± standard error of the mean. ***P<0.001 vs. control. N, neural; E, epithelial; HIF-1α, hypoxia inducible factor-1α; NC, negative control; $CoCl_2$, cobalt II chloride.

treated by $CoCl_2$ has not yet been verified. The content of Notch1 was detected in MiaPaCa2 cells following treatment with $CoCl_2$. It was observed that the transcriptional and translational expression of Notch1 increased in MiaPaCa2 cells treated with $CoCl_2$ (Fig. 5). Additionally, HIF-1α siRNA had the ability to inhibit the expression of Notch1. Therefore,

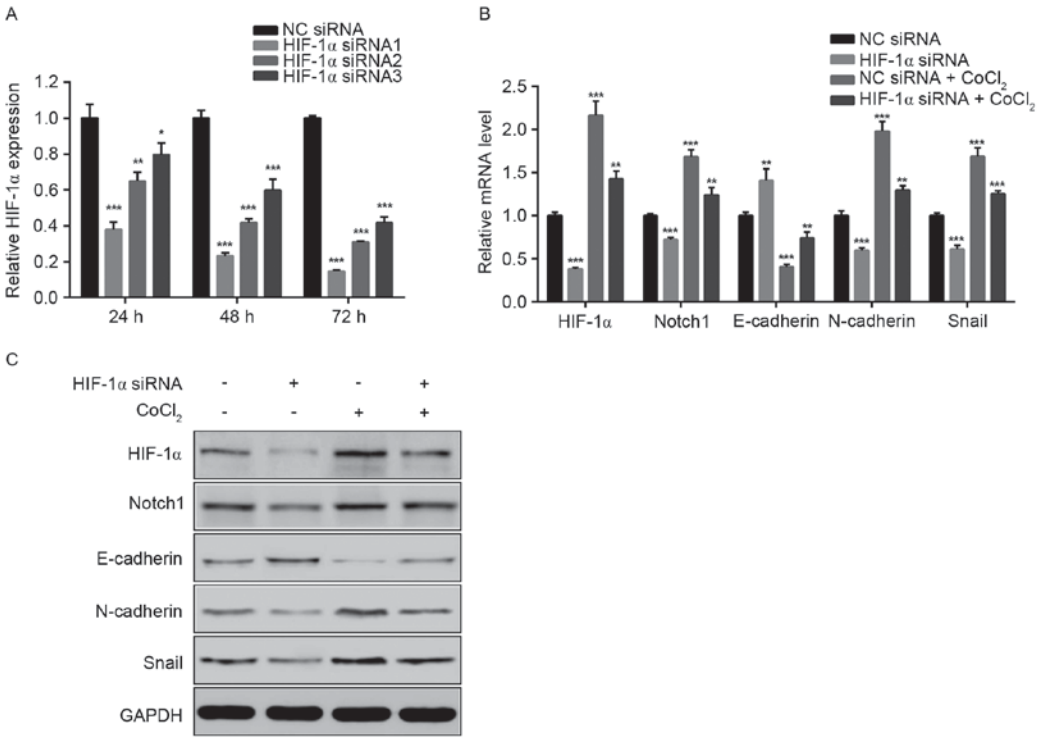

Figure 3. Effects of HIF-1α siRNA on epithelial-mesenchymal transition in MiaPaCa2 cells treated with $CoCl_2$. (A) HIF-1α siRNA was selected by RT-qPCR in MiaPaCa2 cells following transfection with three different HIF-1α siRNA or NC siRNA for 24, 48 and 72 h. (B) The mRNA expression levels of E-cadherin, N-cadherin, Snail, HIF-1α, Notch1 were detected using RT-qPCR in MiaPaCa2 cells treated with or without $CoCl_2$ for 24 h in the presence or absence of HIF-1α siRNA. (C) The protein content of E-cadherin, N-cadherin, Snail, HIF-1α, Notch1 was detected by western blotting in MiaPaCa2 cells treated with or without $CoCl_2$ for 24 h in the presence or absence of HIF-1α siRNA. GAPDH was included as mRNA-loading and protein-loading control. *P<0.05, **P<0.01, ***P<0.001. si, small interfering; RT-qPCR, reverse transcription-quantitative polymerase chain reaction; HIF-1α, hypoxia inducible factor-1α; NC, negative control; E, epithelial; N, neural; $CoCl_2$, cobalt II chloride.

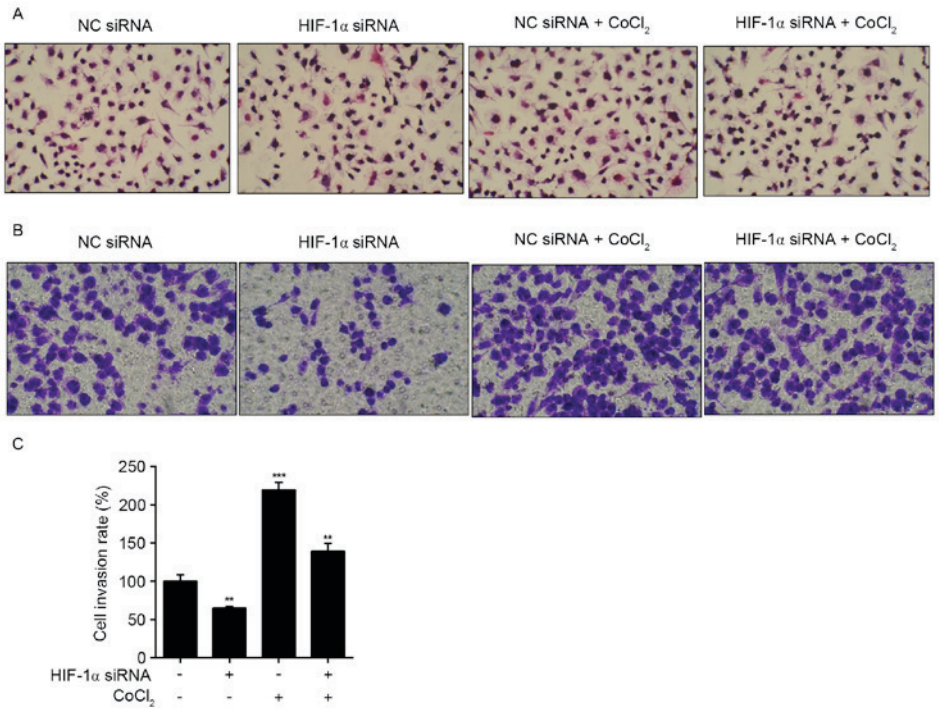

Figure 4. Effects of HIF-1α siRNA on morphology and invasion in MiaPaCa2 cells treated with $CoCl_2$. (A) The morphology of cells was detected by hematoxylin and eosin staining and observed from five randomly selected microscopic visual fields (magnification, x200) following treatment with or without $CoCl_2$ for 24 h in the presence or absence of HIF-1α siRNA. (B) Cell invasion was detected in MiaPaCa2 cells following treatment with or without $CoCl_2$ for 24 h in the presence or absence of HIF-1α siRNA. Invaded cells were stained with crystal violet and observed from five randomly selected microscopic visual fields (magnification, x200). (C) Number of invaded cells were counted and expressed as cell invasion rate (%) compared with those untreated cells without $CoCl_2$ or HIF-1α siRNA. Data were representative of three independent experiments and expressed as the mean ± standard error of the mean. **P<0.01, ***P<0.001. HIF-1α, hypoxia inducible factor-1α; si, small interfering; NC, negative control; $CoCl_2$, cobalt II chloride.

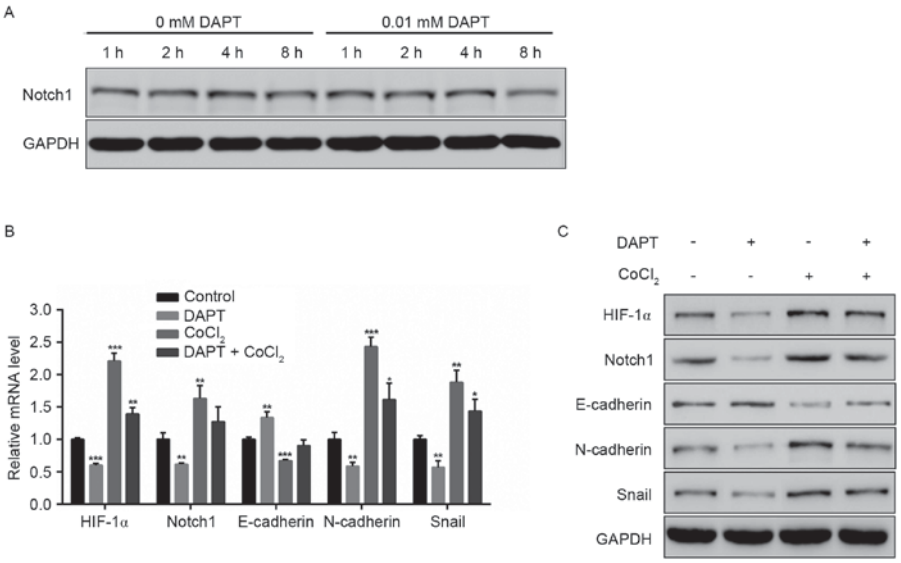

Figure 5. Effects of DAPT on epithelial-mesenchymal transition in MiaPaCa2 cells treated with $CoCl_2$. (A) The expression of Notch1 was measured by western blotting in MiaPaCa2 cells in the presence or absence of DAPT for 1, 2, 4 and 8 h. (B) mRNA expression levels of E-cadherin, N-cadherin, Snail, HIF-1α, Notch1 were detected using RT-qPCR in MiaPaCa2 cells treated with or without $CoCl_2$ for 24 h in the presence or absence of DAPT. (C) The protein content of E-cadherin, N-cadherin, Snail, HIF-1α, Notch1 was detected by western blotting in MiaPaCa2 cells treated with or without $CoCl_2$ for 24 h in the presence or absence of DAPT. GAPDH was included as mRNA-loading and protein-loading control. *P<0.05, **P<0.01, ***P<0.001. RT-qPCR, reverse transcription-quantitative polymerase chain reaction; HIF-1α, hypoxia inducible factor-1α; NC, negative control; E, epithelial; N, neural; DAPT, N-[N-(3,5-Difluorophenacetyl)-L-alanyl]-S-phenylglycine t-butyl ester; $CoCl_2$, cobalt II chloride.

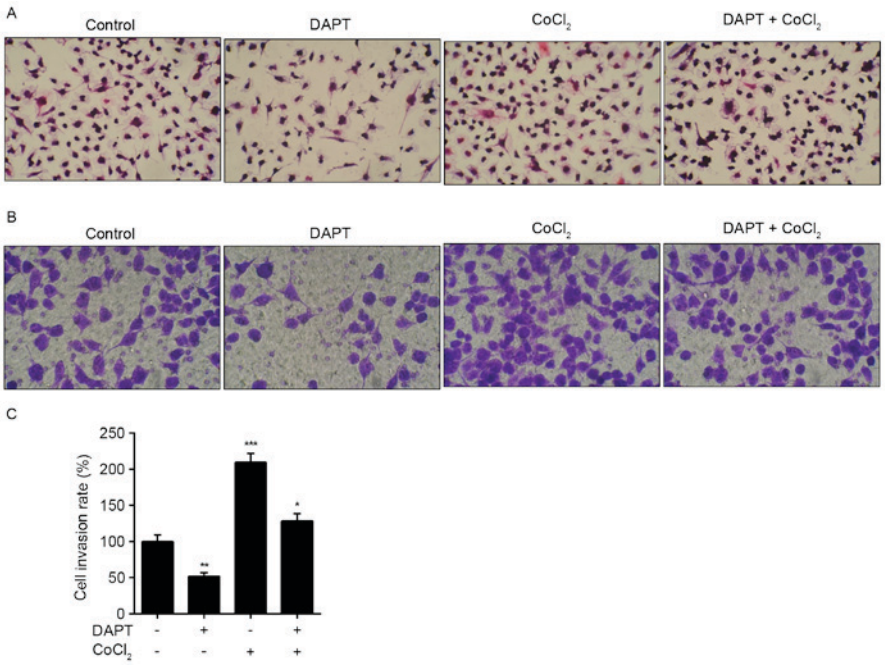

Figure 6. Effects of DAPT on morphology and invasion in MiaPaCa2 cells treated with $CoCl_2$. (A) The morphology of cells was detected by hematoxylin and eosin staining and observed from five randomly selected microscopic visual fields (magnification, x200) following treatment with or without $CoCl_2$ for 24 h in the presence or absence of DAPT. (B) Cell invasion was detected in MiaPaCa2 cells following treatment with or without $CoCl_2$ for 24 h in the presence or absence of DAPT. Invaded cells were stained with crystal violet and observed from five randomly selected microscopic visual fields (magnification, x200). (C) Invaded cells were counted and expressed as cell invasion rate (%) compared with those untreated cells without $CoCl_2$ or DAPT. Data were representative of three independent experiments and expressed as the mean ± standard error of the mean. *P<0.05, **P<0.01, ***P<0.001. DAPT, N-[N-(3,5-Difluorophenacetyl)-L-alanyl]-S-phenylglycine t-butyl ester; $CoCl_2$, cobalt II chloride.

HIF-1α induced by $CoCl_2$, regulated the expression of Notch1. However, it was unclear whether Notch1 was associated with the promotion of EMT and invasion stimulated by $CoCl_2$ in MiaPaCa2 cells. A type of inhibitor designated DAPT, which could repress the activation of Notch signal pathway, was used in MiaPaCa2 cells in the presence or absence of $CoCl_2$. Data demonstrated that DAPT (0.01 mM) inhibited the content of Notch1 following treatment for 8 h in MiaPaCa2 cells, which

restrained EMT and invasion (Fig. 5). Therefore, Notch1 serves an important role in the regulation of EMT and invasion in MiaPaCa2 cells. The results of the present study suggested that $CoCl_2$ may increase cell viability and spindle shape, to favor the promotion of EMT and cell invasion. Additionally, DAPT had the ability to reverse the increase of cell viability and spindle shape induced by $CoCl_2$ (Fig. 6).

Discussion

Cellular metabolism associated with cell proliferation, anti-apoptosis, metastasis and resistance is abnormal in tumorigenesis, probably resulting from the regulation of Wnt/β-catenin pathway, mitogen-activated protein kinase signaling pathway and other signaling pathways, and hypoxia has an important role in this process (26,27). It has been reported that hypoxia is also able to maintain the characteristic of cancer stem cells and induce the progression of cancer cells (28). Pancreatic cancer possesses the characteristics of a solid tumor and hypoxia also exists in pancreatic cancer (29), however the mechanism involved in the pathogenesis of pancreatic cancer remains unclear. In the present study, Mia-PaCa2 cells, a pancreatic cancer cell line with high rate of metastasis, were used to investigate the effects and mechanism of hypoxia on pancreatic cancer cells.

The CCK-8 assay demonstrated that $CoCl_2$ (0.08 mM) increased the invasion rate by two-fold in MiaPaCa2 cells, whereas $CoCl_2$ at this concentration had a mild effect on the growth of MiaPaCa2 cells. The invasion ability is different between mesenchymal cells and epithelial cells resulting from differences in the cytoskeleton. The results of the present study indicated that $CoCl_2$ altered cell morphology to spindle shaped, which is similar to that of mesenchymal cells and the expression of E-cadherin and N-cadherin was altered in MiaPaCa2 cells treated with $CoCl_2$ on a transcriptional and translational level. An increase in invasion in MiaPaCa2 cells may be induced by $CoCl_2$ and results in EMT. It has been reported that Snail, a transcription factor, combines with E-cadherin and inhibits the transcriptional activity of E-cadherin, leading to a promotion to EMT in pancreatic cancer (30-33). The content of Snail increased in MiaPaCa2 cells in the presence of $CoCl_2$ in the present study.

To identify if $CoCl_2$ could act as hypoxia inducer, HIF-1α, which is induced by hypoxia, was detected in MiaPaCa2 cells treated with $CoCl_2$. The present study demonstrated that $CoCl_2$ promoted the expression level of HIF-1α. The results demonstrated that HIF-1α siRNA reversed the increase in the expression of Snail, EMT and invasion induced by $CoCl_2$ in MiaPaCa2 cells. This indicated that $CoCl_2$ simulated hypoxia, which induced the expression of HIF-1α and increased the expression of Snail, and then promoted EMT leading to an increase to invasion.

Furthermore, the mechanism by which HIF-1α regulates the expression of Snail and EMT was also investigated in the present study. It has been reported that the Notch signaling pathway is involved in EMT and HIF-1α is able to regulate its activation in cancer cells (20,21). The present study demonstrated that $CoCl_2$ increased the expression of Notch1, which was associated with an increase to transcriptional expression. DAPT targeted Notch1 and inhibited the function of Notch1 leading to an inhibition of the signaling pathway and decreased expression of Snail, EMT and cell invasion in MiaPaCa2 cells, induced by $CoCl_2$. In addition, HIF-1α siRNA also possessed the ability to repress the expression of Notch1. Therefore, $CoCl_2$ induced the expression of HIF-1α, stimulated the activation of Notch1 signal molecule, and then increased the expression of Snail at a transcriptional and translational level, leading to a promotion of EMT and an increase in invasion of MiaPaCa2 cells. Targeting Notch1 is a potential treatment strategy to inhibit the increase in EMT and invasion induced by hypoxia.

In conclusion, DAPT regulated the expression of HIF-1α at a transcriptional and translational level, which suggests the existence of a feedback loop in the HIF-1α/Notch1 signaling pathway. Additionally, EMT is associated with cancer stem cells, which control recurrence (34). DAPT may also have the ability to inhibit the recurrence of pancreatic cancer by regulating EMT and affecting the behaviors of cancer stem cells, however further investigation is required. DAPT or other inhibitors of Notch1 signaling molecule may have potential in the treatment of pancreatic cancer in the future.

Acknowledgements

The present study was supported by grant from Natural Science Foundation of Zhejiang Province (grant no. LY12H16026).

References

1. Ryan DP, Hong TS and Bardeesy N: Pancreatic adenocarcinoma. N Engl J Med 371: 1039-1049, 2014.
2. Zell JA, Rhen JM, Ziogas A, Lipkin SM and Anton-Culver H: Race, socioeconomic status, treatment, and survival time among pancreatic cancer cases in California. Cancer Epidemiol Biomarkers Prev 16: 546-552, 2007.
3. Lau MK, Davila JA and Shaib YH: Incidence and survival of pancreatic head and body and tail cancers: A population-based study in the United States. Pancreas 39: 458-462, 2010.
4. Quaresma M, Coleman MP and Rachet B: 40-year trends in an index of survival for all cancers combined and survival adjusted for age and sex for each cancer in England and Wales, 1971-2011: A population-based study. Lancet 385: 1206-1218, 2015.
5. Siegel RL, Miller KD and Jemal A: Cancer statistics, 2015. CA Cancer J Clin 65: 5-29, 2015.
6. Yasuda H: Solid tumor physiology and hypoxia-induced chemo-radio-resistance: Novel strategy for cancer therapy: Nitric oxide donor as a therapeutic enhancer. Nitric Oxide 19: 205-216, 2008.
7. Silva P, Mendoza P, Rivas S, Díaz J, Moraga C, Quest AF and Torres VA: Hypoxia promotes Rab5 activation, leading to tumor cell migration, invasion and metastasis. Oncotarget 7: 29548-29562, 2016.
8. Rohwer N and Cramer T: Hypoxia-mediated drug resistance: Novel insights on the functional interaction of HIFs and cell death pathways. Drug Resist Updat 14: 191-201, 2011.
9. Trédan O, Galmarini CM, Patel K and Tannock IF: Drug resistance and the solid tumor microenvironment. J Natl Cancer Tnst 99: 1441-1454, 2007.
10. Zhao Q, Tan BB, Li Y, Fan LQ, Yang PG and Tian Y: Enhancement of Drug Sensitivity by Knockdown of HIF-1α in gastric carcinoma cells. Oncol Res 23: 129-136, 2016.
11. Koukourakis MI, Kakouratos C, Kalamida D, Bampali Z, Mavropoulou S, Sivridis E and Giatromanolaki A: Hypoxia-inducible proteins HIF1α and lactate dehydrogenase LDH5, key markers of anaerobic metabolism, relate with stem cell markers and poor post-radiotherapy outcome in bladder cancer. Int J Radiat Biol 92: 353-363, 2016.
12. Joshi S, Kumar S, Ponnusamy MP and Batra SK: Hypoxia-induced oxidative stress promotes MUC4 degradation via autophagy to enhance pancreatic cancer cells survival. Oncogene 35: 5882-5892, 2016.

13. Rani A and Prasad S: CoCl2-induced biochemical hypoxia down regulates activities and expression of super oxide dismutase and catalase in cerebral cortex of mice. Neurochem Res 39: 1787-1796, 2014.
14. Yang G, Xu S, Peng L, Li H, Zhao Y and Hu Y: The hypoxia-mimetic agent $CoCl_2$ induces chemotherapy resistance in LOVO colorectal cancer cells. Mol Med Rep 13: 2583-2589, 2016.
15. Pang MF, Georgoudaki AM, Lambut L, Johansson J, Tabor V, Hagikura K, Jin Y, Jansson M, Alexander JS, Nelson CM, *et al*: TGF-β1-induced EMT promotes targeted migration of breast cancer cells through the lymphatic system by the activation of CCR7/CCL21-mediated chemotaxis. Oncogene 35: 748-760, 2016.
16. Yilmaz M and Christofori G: EMT, the cytoskeleton, and cancer cell invasion. Cancer Metastasis Rev 28: 15-33, 2009.
17. Zhang W, Shi X, Peng Y, Wu M, Zhang P, Xie R, Wu Y, Yan Q, Liu S and Wang J: HIF-1α promotes epithelial-mesenchymal transition and metastasis through direct regulation of ZEB1 in colorectal cancer. PLoS One 10: e0129603, 2015.
18. Cho KH, Choi MJ, Jeong KJ, Kim JJ, Hwang MH, Shin SC, Park CG and Lee HY: A ROS/STAT3/HIF-1α signaling cascade mediates EGF-induced TWIST1 expression and prostate cancer cell invasion. Prostate 74: 528-536, 2014.
19. Luo Y, Lan L, Jiang YG, Zhao JH, Li MC, Wei NB and Lin YH: Epithelial-mesenchymal transition and migration of prostate cancer stem cells is driven by cancer-associated fibroblasts in an HIF-1α/β-catenin-dependent pathway. Mol Cells 36: 138-144, 2013.
20. Hu YY, Fu LA, Li SZ, Chen Y, Li JC, Han J, Liang L, Li L, Ji CC, Zheng MH and Han H: Hif-1α and Hif-2α differentially regulate Notch signaling through competitive interaction with the intracellular domain of Notch receptors in glioma stem cells. Cancer Lett 349: 67-76, 2014.
21. Tian Q, Xue Y, Zheng W, Sun R, Ji W, Wang X and An R: Overexpression of hypoxia-inducible factor 1α induces migration and invasion through Notch signaling. Int J Oncol 47: 728-738, 2015.
22. Giachino C, Boulay JL, Ivanek R, Alvarado A, Tostado C, Lugert S, Tchorz J, Coban M, Mariani L, Bettler B, *et al*: A tumor suppressor function for Notch signaling in forebrain tumor subtypes. Cancer Cell 28: 730-742, 2015.
23. Zhou J, Jain S, Azad AK, Xu X, Yu HC, Xu Z, Godbout R and Fu Y: Notch and TGFβ form a positive regulatory loop and regulate EMT in epithelial ovarian cancer cells. Cell Signal 28: 838-849, 2016.
24. Ishida T, Hijioka H, Kume K, Miyawaki A and Nakamura N: Notch signaling induces EMT in OSCC cell lines in a hypoxic environment. Oncol Lett 6: 1201-1206, 2013.
25. Livak KJ and Schmittgen TD: Analysis of relative gene expression data using real-time quantitative PCR and the 2(-Delta Delta C(T)) method. Methods 25: 402-408, 2001.
26. Braunschweig L, Meyer AK, Wagenführ L and Storch A: Oxygen regulates proliferation of neural stem cells through Wnt/β-catenin signalling. Mol Cell Neurosci 67: 84-92, 2015.
27. Qiu Y, Chen Y, Zeng T, Guo W, Zhou W and Yang X: High mobility group box-B1 (HMGB1) mediates the hypoxia-induced mesenchymal transition of osteoblast cells via activating ERK/JNK signaling. Cell Biol Int 40: 1152-1161, 2016.
28. Xie J, Xiao Y, Zhu XY, Ning ZY, Xu HF and Wu HM: Hypoxia regulates stemness of breast cancer MDA-MB-231 cells. Med Oncol 33: 42, 2016.
29. Li H, Li J, Liu X, Chen J, Wu C and Guo X: Effect of PTEN and KAI1 gene overexpression on the proliferation, metastasis and radiosensitivity of ASPC-1 pancreatic cancer cells under hypoxic conditions. Mol Med Rep 10: 1973-1977, 2014.
30. Kang H, Lee M and Jang SW: Celastrol inhibits TGF-β1-induced epithelial-mesenchymal transition by inhibiting Snail and regulating E-cadherin expression. Biochem Biophys Res Commun 437: 550-556, 2013.
31. Galván JA, Zlobec I, Wartenberg M, Lugli A, Gloor B, Perren A and Karamitopoulou E: Expression of E-cadherin repressors SNAIL, ZEB1 and ZEB2 by tumour and stromal cells influences tumour-budding phenotype and suggests heterogeneity of stromal cells in pancreatic cancer. Br J Cancer 112: 1944-1950, 2015.
32. Ji Q, Liu X, Han Z, Zhou L, Sui H, Yan L, Jiang H, Ren J, Cai J and Li Q: Resveratrol suppresses epithelial-to-mesenchymal transition in colorectal cancer through TGF-β1/Smads signaling pathway mediated Snail/E-cadherin expression. BMC Cancer 15: 97, 2015.
33. Xu X, Tan X, Tampe B, Sanchez E, Zeisberg M and Zeisberg EM: Snail Is a direct target of hypoxia-inducible factor 1α (HIF1α) in hypoxia-induced endothelial to mesenchymal transition of human coronary endothelial cells. J Biol Chem 290: 16653-16664, 2015.
34. Wen Z, Feng S, Wei L, Wang Z, Hong D and Wang Q: Evodiamine, a novel inhibitor of the Wnt pathway, inhibits the self-renewal of gastric cancer stem cells. Int J Mol Med 36: 1657-1663, 2015.

This work is licensed under a Creative Commons Attribution-NonCommercial-NoDerivatives 4.0 International (CC BY-NC-ND 4.0) License.